Journal of Science: Advanced Materials and Devices 8 (2023) 100638

Contents lists available at ScienceDirect

Journal of Science: Advanced Materials and Devices

journal homepage: www.elsevier.com/locate/jsamd

Original Article

Surface modified carbon nanotubes fiber as flexible bifunctional electrocatalyst for overall electrochemical water splitting reactions

Haia Aldosari [a], Abid Ali [b,*], Muhammad Adeel Asghar [b,**], Ali Haider [c], Yasir Mehmood [d], Zafar Iqbal [e], Arif Nazir [b], Munawar Iqbal [f]

[a] Department of Physics, College of Science, Shaqra University, P.O. Box 5701, Shaqra, 11961, Saudi Arabia
[b] Department of Chemistry, The University of Lahore, 1-Km Defence Road, Lahore 54590, Pakistan
[c] Department of Chemistry, Quaid-i-Azam University Islamabad 45320, Pakistan
[d] Department of Chemistry, Abbottabad University of Science and Technology, 22500 Abbottabad, Pakistan
[e] Helmholtz-Zentrum Berlin für Materialien und Energie GmbH, Hahn-Meitner-Platz 1, 14109 Berlin, Germany
[f] Department of Chemistry, Division of Science and Technology, University of Education, Lahore, Pakistan

ARTICLE INFO

Keywords:
CoSe nanoparticles
CNTs fiber
Electrocatalysis
Water splitting
Flexibility

ABSTRACT

Electrocatalytic water splitting is regarded as a promising approach to produce hydrogen, which is a clean and renewable fuel. The process is mainly constrained due to the sluggish proton-coupled four-electrode transfer process at the anode for oxygen evolution reaction (OER) with high overpotential requirement. Herein this work, we used a one-step hydrothermal method for the in-situ synthesis of CoSe nanoparticles over the surface of carbon nanotube-based fiber (CNTs fiber) and utilized it as a bifunctional electrocatalyst for the electrochemical water splitting process. Surface-modified fiber showed excellent performance towards OER with a low overpotential (η_{10} = 414 mV) and Tafel slope (77 mVdec^{-1}). We also exploited the same material as cathode, which exhibited an excellent hydrogen evolution reaction (HER) at the counterpart with improved catalytic performance as compared to bare CNTs materials. During the HER process in the cathodic potential region, the electrocatalyst displayed a current density of 10 mAcm^{-2} at an overpotential of 496 mV. Furthermore, the electrocatalyst exhibited excellent performance during the testing for the overall water splitting. The outcomes reveal that the fabricated electrode can be potentially applied as an efficient and flexible electrode to derive the hydrogen as fuels during the overall electrochemical water splitting reaction.

1. Introduction

The rapid depletion of fossil fuels and their environmentally hazardous effects compelled researchers to seek reliable and cleaner alternative energy resources [1–3]. Reliance on renewable energy sources such as solar and wind energy is hindered due to the intermittent nature of these sources [4–6]. The need for incessant utilization of these energy sources led to electrocatalytic water splitting as an attractive and environmentally friendly route for large-scale hydrogen production [7–9]. Both non-renewable and renewable sources can be utilized to drive the water electrolysis reaction for the generation of hydrogen through the cathodic HER and anodic OER. However, in comparison with the efficient rate of the two-electron transfer pathway of HER, the sluggish kinetics of the proton-coupled four-electron transfer mechanism of OER impede the process of generating hydrogen fuels smoothly [10,11].

RuO_2 and IrO_2 are the benchmark catalysts used to minimize the energy barrier for OER [12–14]. They are quite expensive and scarce, which hinders their large-scale utilization. Corrosion and dissolution during OER reactions are other problems associated with these materials [13,15]. Therefore, significant research efforts have been made on the improvement of cheap metal-based OER electrocatalysts employing earth-abundant metals or using their derivatives [16–18]. In this respect, the first-row transition metals-based electrocatalysts OER have been efficiently employed by various research groups [19,20]. Within the non-metallic domain, carbon-based materials and their composites like carbon fibers, carbon nanotubes and graphene are among the most

Peer review under responsibility of Vietnam National University, Hanoi.
* Corresponding author.
** Corresponding author. Department of Chemistry, The University of Lahore, 1-Km Defence Road, Lahore 54590, Pakistan.
E-mail addresses: abid.ali@chem.uol.edu.pk (A. Ali), madeelchem@gmail.com (M.A. Asghar).

https://doi.org/10.1016/j.jsamd.2023.100638
Received 1 June 2023; Received in revised form 13 September 2023; Accepted 23 September 2023
Available online 28 September 2023

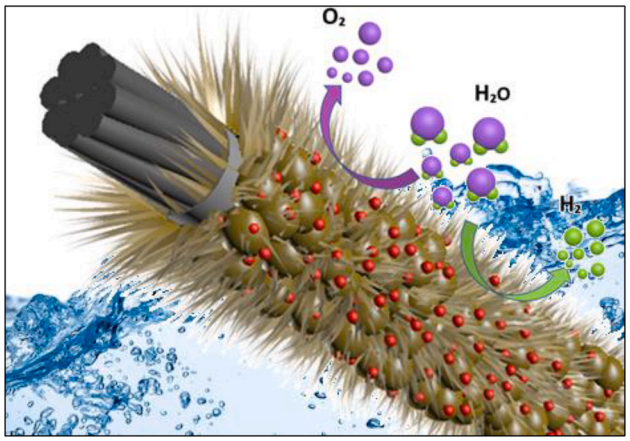

Fig. 1. Schematic illustration of CoSe@CNTs fiber electrode for overall electrochemical water splitting.

promising electrocatalysts for water splitting [21–26]. Carbon nanotubes and graphene have been widely used with transition metals-based alloys [26–28], oxides [29–31], sulfides [32–34] and selenides [35–39] for electrochemical water splitting. These composites not only exhibit the features of their individual components but also new physical and chemical properties are originated by the synergistic impact of carbon materials together with transition metals resulting in higher activity towards electrochemical water splitting reactions [21,23,32,40,41]. Recently, metal selenide-based carbon nanocomposites were used as electrocatalysts for water splitting which attracted much attention due to their higher activity, low cost and facile synthesis [42–44]. Carbon materials such as CNTs, graphene and carbon fiber have been widely used in powder form fabricated over glassy carbon electrodes, conducting glass, carbon clothing and nickel foam which hindered their utilization with the binding approach. Of all the known carbon-based materials/composites, carbon fiber cloth is considered a flexible electrode. However, it exhibits low mechanical strength and poor conductivity that hinders its multidirectional applications. To this end, carbon nanotubes in the form of fiber with a high tensile strength of ~100 GPa, electrical conductivity of 10^4 Scm^{-1} and bending stiffness of 0.00176–1.23 nN m^2 could be the promising materials for the electrocatalytic applications [43,45].

Here in this work, we developed flexible CNTs fiber electrode modified with cobalt selenide (CoSe) nanoparticles via a facile in-situ single-step hydrothermal process and utilized it as an efficient electrocatalyst for overall electrochemical water splitting in addition to OER and HER. The fabricated electrode exhibited higher electrocatalytic activity and better stability as compared to other carbon-based materials. Cyclic processes in CV and chronoamperometric studies showed splendid stability with time, which could make these materials superior for the overall electrochemical water splitting reaction along with OER. A schematic illustration is shown in Fig. 1, showing the modified CNTs fiber for overall electrochemical water spelling reactions.

2. Experimental

2.1. Growth of MWCNTs arrays

A previously reported chemical vapor deposition (CVD) method was adopted for the fabrication of highly aligned spinnable multiwalled carbon nanotubes (MWCNTs) which is schematically illustrated in Fig. 2 [46]. Briefly, alumina (Al_2O_3) acting as a buffer layer was deposited on a silicon wafer substrate via the physical vapor deposition (PVD) method at very low pressure. A thin film of iron (Fe) was also deposited via the PVD method over the surface of the alumina layer and annealed subsequently. Upon annealing, Fe thin film formed iron nanoparticles that acted as a catalyst for the growth of MWCNTs arrays. Ethylene in combination with hydrogen and argon were used as a precursor and source gases, respectively, with the flow rate of 90, 30 and 400 sccm (standard cubic centimeter per minute), in a quartz tube furnace with the temperature maintained at 740 °C.

2.2. Spinning of fiber from arrays

MWCNTs arrays formed were drawn as sheets with a fine edge blade and spun into CNTs fiber using a microprobe rotating at a speed of 2000 rpm (see Fig. 2). This fiber was then attached to a glass support through Teflon tape. A video demonstrating the sheet extraction and spinning into CNTs fiber is also provided in supporting information.

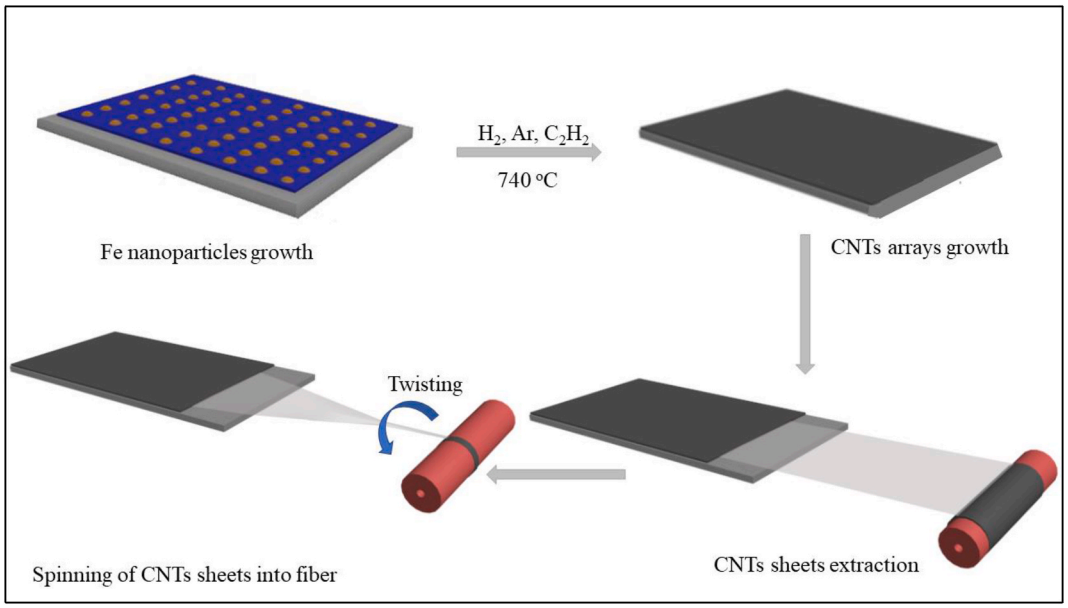

Fig. 2. Schematic illustration of CNTs sheets extraction and spinning into fiber.

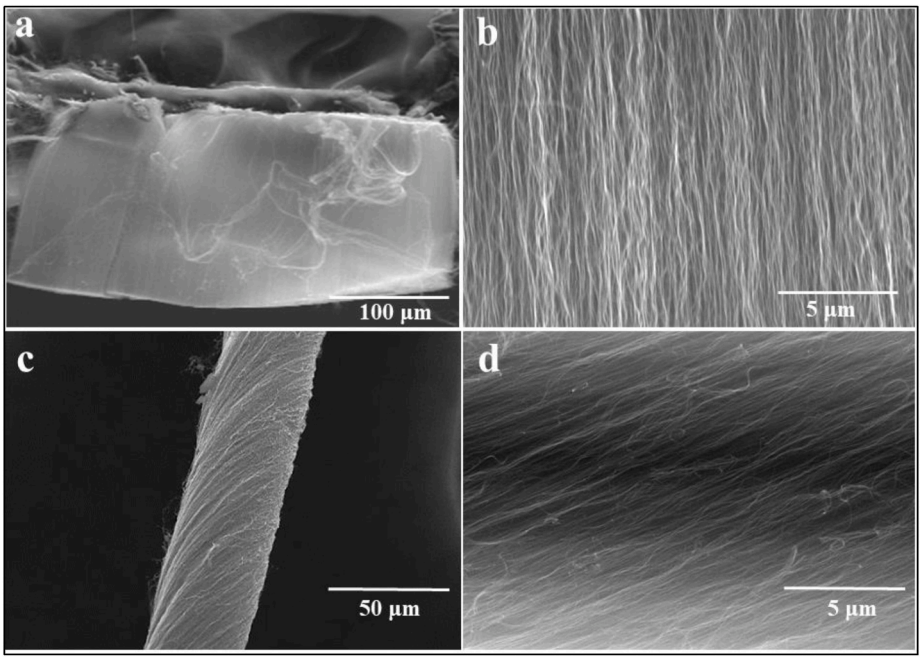

Fig. 3. SEM images of **(a, b)** CNTs arrays and **(c, d)** bare CNTs fiber at lower and higher magnification.

2.3. Surface modification of MWCNTs fiber with CoSe

In situ surface modification of CNTs fiber with CoSe was obtained using the hydrothermal method. Briefly, 124.5 mg (0.5 mmol) of cobalt (II) acetate tetrahydrate ($Co(OOCCH_3)_2 \cdot 4H_2O$) was dissolved in 10 ml of deionized water with mechanical stirring. Then 55.3 mg (0.7 mmol) of Se powder was added to the stirring solution followed by the dropwise addition of 5 ml hydrazine. A single CNTs fiber with a diameter of ~40 µm and a length of 3 cm was attached to the glass substrate that was transferred to a 25 ml Teflon lined autoclave containing reaction mixture followed by heating in a furnace at 180 °C for 16 h. After cooling down to room temperature, the fiber was washed with deionized water and ethanol several times and finally dried at 60 °C overnight. The Teflon was then removed, and an electrical connection was established using silver paste.

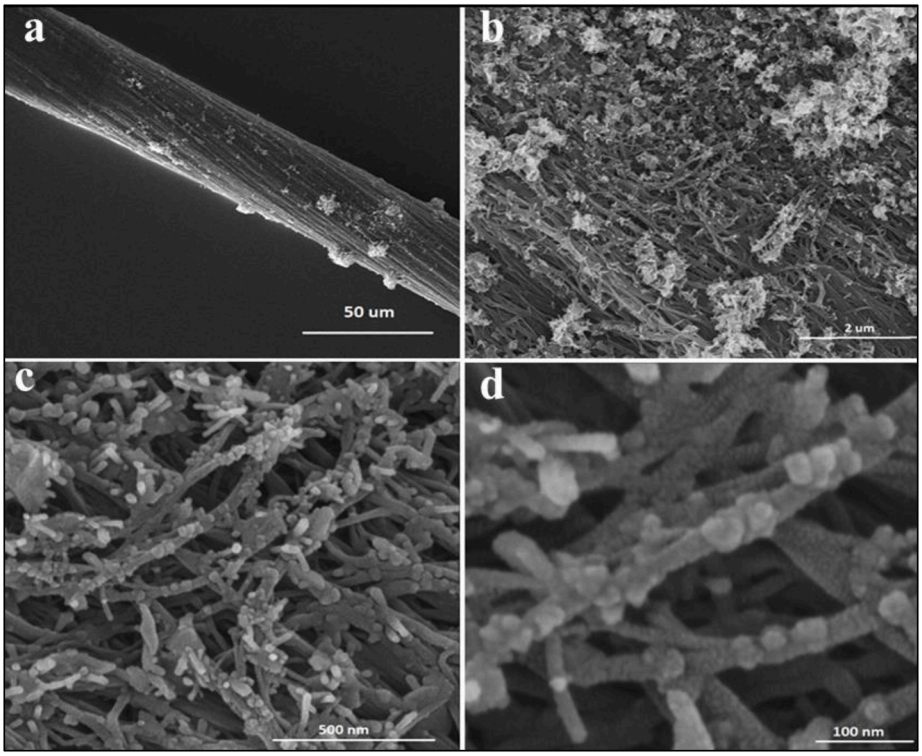

Fig. 4. SEM images of the CoSe@CNTs fibers with **(a, b)** lower and **(c, d)** higher magnifications.

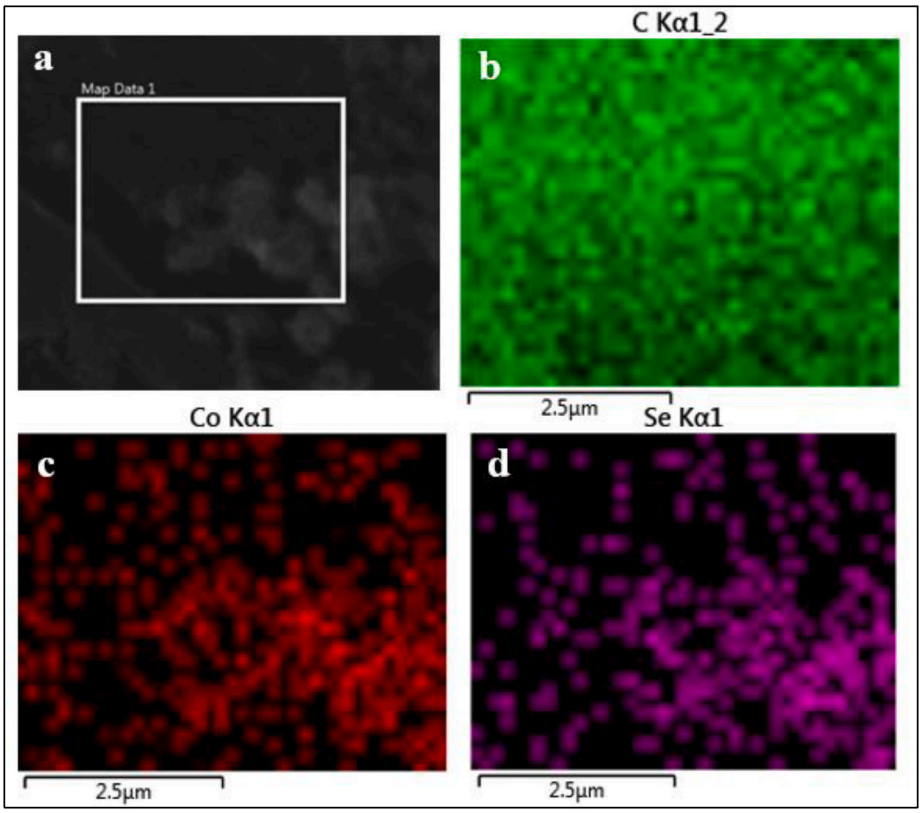

Fig. 5. **(a)** SEM image and EDX for the elemental mapping of **(b)** carbon **(c)** cobalt and **(d)** selenium over the surface of CNTs fiber.

2.4. Material characterization

Scanning electron microscopy (SEM) and energy dispersive X-ray spectroscopy (EDS) analyses were acquired using Quanta FEG250, Bruker. The microscope was operated at an acceleration voltage of 5 kV. All electrochemical studies were carried out using the Gamry Interface 1010 E Potentiostat/Galvanostat with current-interpret *iR* compensation.

2.5. Electrochemical measurements

All electrochemical studies were carried out in a three-electrode setup with CoSe@CNTs fiber as a working electrode while silver-silver chloride (Ag/AgCl) and Pt wire electrodes were used as reference and counter electrodes, respectively in 1.0 M KOH ($pH = 13$). Measured potentials against Ag/AgCl were converted to RHE using equation (2.1).

$$E_{RHE} = E_{Ag/AgCl} + 0.197 + 0.059 \times pH \quad 2.1$$

Linear sweep voltammetry (LSV) of the samples was performed between 0 and 1 V vs. Ag/AgCl at a scan rate of 5 mVs^{-1}. Cyclic voltammetry (CV) was recorded in the non-faradaic region to investigate the electrochemical surface area (ECSA). Chronoamperometric measurements for CoSe@CNTs fiber electrode were measured in 1.0 M KOH for 10 h at the potential corresponding to 10 $mAcm^{-2}$ current density. Electrochemical impedance spectroscopy (EIS) measurements were carried out over a frequency range from 1 MHz to 0.1 Hz and a sinusoidal voltage amplitude of 5 mV in the region of faradaic DC voltage. Overall electrochemical water splitting was carried out with the two-electrode setup. To obtain the current density, all the current values were normalized with respect to the geometrical surface area of the working electrode. All the electrochemical measurements were recorded at room temperature (25 °C).

3. Results and discussion

3.1. Surface morphology and elemental mapping

SEM images were obtained at different magnifications to probe the surface morphology of CNTs arrays and fibers. Vertically aligned CNTs grown over the surface of silicon substrate have unique structure as shown in Fig. 3 (a, b). Images at low and high resolution illustrated the aligned structure of arrays with the nano-sized diameter and several millimeters of length. Fig. 3 (c, d) shows the spun fiber with several units of CNTs with a diameter of ~40 μm. A magnified view of the CNTs fiber shown in Fig. 3(b) displayed the further in-depth exploration with numerous CNTs fibrous-like units. A single unit of CNTs fiber demonstrated a diameter in the range of 15–20 nm as shown in Fig. S1 in supporting information. These unidirectional CNTs fibers play a significant role in the smooth flow of charge transportation. The diameter of the CNTs fiber could be controlled by the additional number of sheets while spinning into fiber. As fabricated fiber could be easily knitted within the fabric (Fig. S2) which indicates this material as a vital candidate for the flexible energy harvesting system.

Surface modification of CNTs fiber with CoSe nanoparticles was carried out via a simple one-step hydrothermal process. The SEM analysis shows the successful growth of CoSe nanoparticles over the CNTs fiber surface (Fig. 4). SEM images at different magnifications (50 μm–100 nm) showed the thorough probe from the diameter (~30 μm) of the fiber based modified electrode to CoSe nanoparticles (20–30 nm). CoSe nanoparticles grown over the surface of CNTs fiber provide the active sites during the catlytic process while fiber offers the flow path for charge transportation.

Energy dispersive X-ray spectroscopy (EDS) was performed for the confirmation of elements (Co and Se) deposited over the fiber surface. Fig. 5(a) shows the SEM image of a small portion of CNTs fiber and their respective elemental mapping of different distributions. Fig. 5 (b) with the deepest green color presented the carbon of CNTs fiber over which

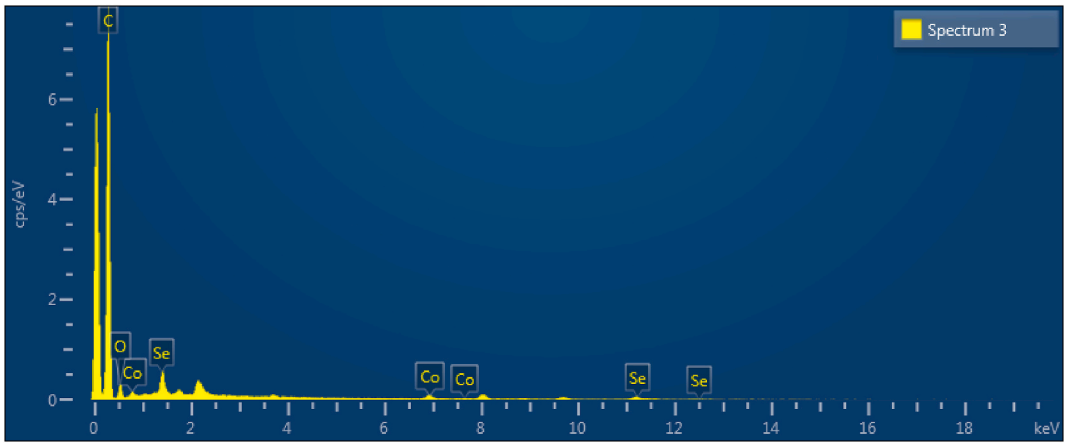

Fig. 6. EDX spectrum for the elemental confirmation of modified CNTs fiber.

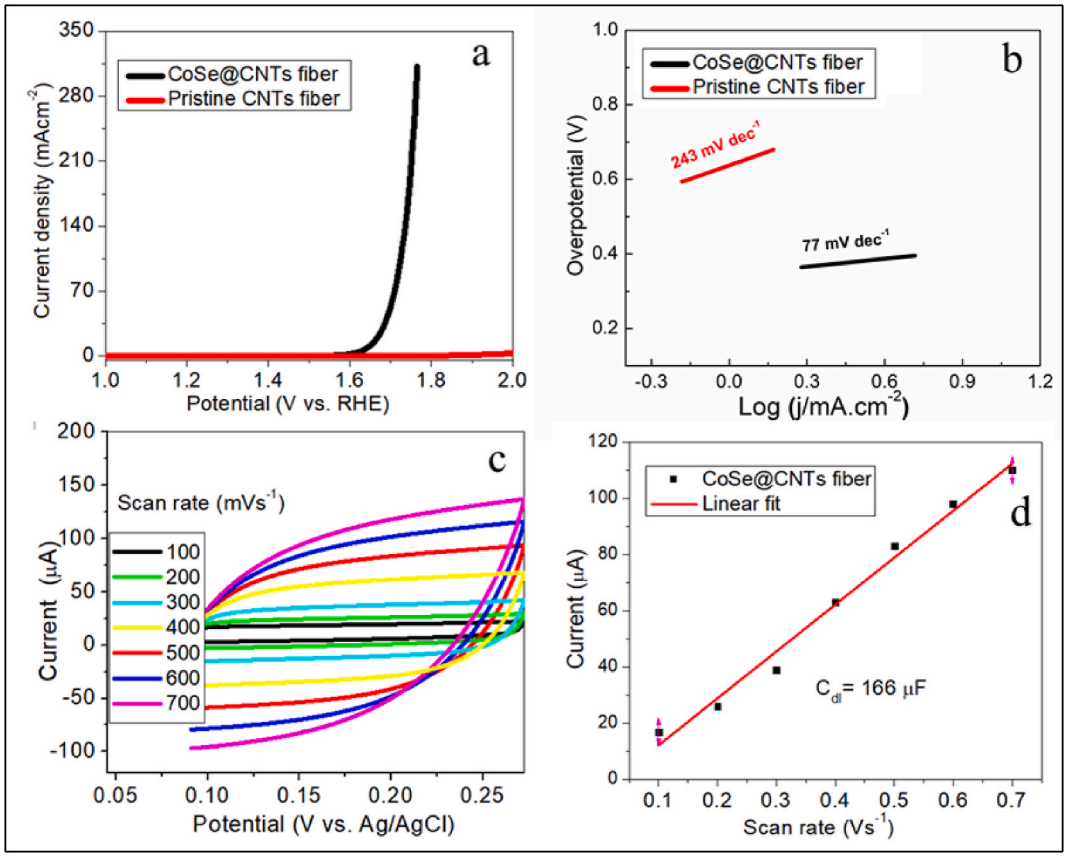

Fig. 7. (a) *iR*-corrected polarization curves and their respective **(b)** Tafel slopes for pristine and CoSe@CNTs fiber for OER in 1 M KOH solution **(c)** cyclic voltammograms of CoSe@CNTs fiber electrode at different scan rates and their **(d)** calibration curves for C_{dl} value.

the deposited Co and Se within the nanoparticles can be seen shown in Fig. 5(c) and (d) with red and violet colors, respectively. Uniform distribution with low density as compared to carbon confirms the deposition of Co and Se over CNTs-based substrate.

The percentage composition of the different elements over the surface of CNTs fiber via EDX analysis has been given in Fig. 6. The high carbon peak along with the peaks of cobalt (Co) and selenium (Se) confirmed the formation of CoSe@CNTs fiber. A small oxygen peak can be attributed to the atmospheric oxygen or oxidized CNTs during the material growth.

3.2. Electrocatalytic activity

3.2.1. Oxygen evolution reaction

Bare and CoSe@CNTs fiber electrodes were investigated for OER activity in basic media. LSV, CV, chronoamperometry and EIS were used to study the overpotential, double-layer capacitance (C_{dl}), stability and charge transfer kinetics, respectively. Fig. 7 (a) shows LSV curves for pristine CNTs fiber and CoSe@CNTs fiber in 1 M KOH solution at a scan rate of 5 mVs^{-1}. CoSe@CNTs fiber electrode achieved the current density of 10 $mAcm^{-2}$ and 100 $mAcm^{-2}$ at the overpotential values of 414 and 494 mV, respectively. In comparison, bare CNTs fiber has very low activity toward electrochemical water oxidation. Evaluation of the Tafel

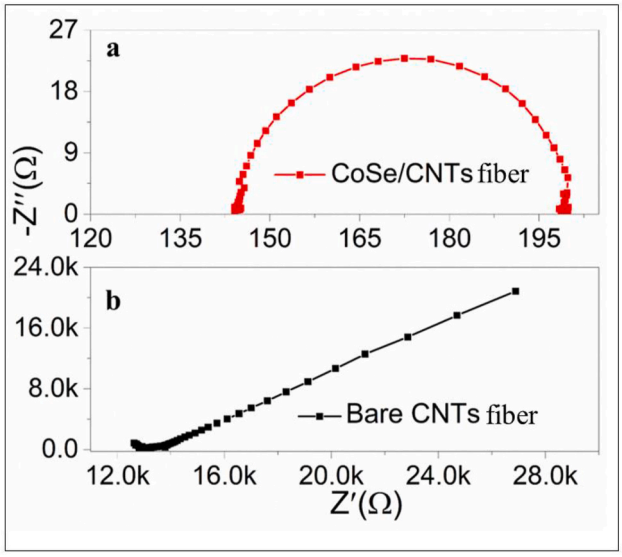

Fig. 8. Nyquist plots for **(a)** CoSe@CNTs fiber and **(b)** bare CNTs fiber electrodes measured in the frequency range of 0.1 Hz–1 MHz.

slope value for CoSe@CNTs fiber (77 $mVdec^{-1}$) with that for bare CNTs fiber (243 $mVdec^{-1}$) and benchmark IrO_2 (~62 $mVdec^{-1}$) [47] confirms the efficient OER electrocatalysis of the modified electrode as given in Fig. 7(b). The C_{dl} of an electrode relates it to the ECSA and describes the active sites of an electrocatalyst. In the non-faradaic potential region, C_{dl} was evaluated for bare and modified electrodes at the scan rates and the plot is shown in Figs. S3(a and b) and 7 (c), respectively. It can be seen from Fig. 7(c) that the charging current also increases with increasing scan rate. The current versus scan rate plot is shown in Fig. 7(d). The modified electrode demonstrated a boosted capacitance of 166 μF $mFcm^{-2}$ as compared to 8.10 μF for pristine CNTs. The ECSA for the modified fiber was calculated to be 4.15 cm^2 which is much higher as compared to that of the pristine CNTs (0.20 cm^2). These results reveal that CoSe@CNTs fiber exhibited improved electrocatalytic activity towards OER due to its enhanced ECSA. An optical image is provided in Fig. S4 demonstrating the electrochemical setup for OER at the modified electrode.

To investigate the insight of OER kinetics, EIS was also performed. The Nyquist plots (obtained via plotting the real and imaginary resistance on abscissa and ordinate, respectively) of CoSe@CNTs fiber and pristine CNTs fiber are presented in Fig. 8(a) and (b), respectively. As anticipated, the CoSe@CNTs fiber has a smaller semicircle diameter in the high-frequency region as compared to that of pristine CNTs fiber that demonstrates smaller charge transfer resistance (~57 Ω) exhibited by CoSe@CNTs fiber. This value is considerably lesser than that for pristine CNTs fiber (1.2 kΩ) implying the faster charge transfer process and hence efficient OER kinetics displayed by CoSe@CNTs fiber electrode.

Long-term electrochemical stability is an important parameter to evaluate the durability of the electrode and is done through chronoamperometric measurements at an applied overpotential of 414 mV (η = 10 $mAcm^{-2}$). It has been found that approximately 90% of the current is maintained after 10 h under alkaline conditions as shown in Fig. 9 (a). Furthermore, the stability of the fabricated electrode has also been checked via CV cycles and the results are shown in Fig. 9(b). Cyclic voltammograms for the CoSe@CNTs fiber electrode maintained the well-conserved current and voltage parameters for 500 cycles. Both amperometric and voltammetric measurements reflected better stability of the electrode which is a vital parameter for practical implementation toward electrochemical water splitting. Various electrochemical parameters for the electrocatalysis of water oxidation and overall water splitting are summarized in Table 1. Comparative data for the different catalysts toward the OER activity has been given in the Table 2 in supporting information. Among all the reported catalysts, CoSe-coated CNTs fiber has remarkable potential to work as a flexible electrode which could be employed in diverse applications.

3.2.2. *Hydrogen evolution reaction*

To be considered as a multipurpose electrocatalyst, hydrogen evolution reaction (HER) has also been investigated for the fabricated electrode in the cathodic potential region in the alkaline media. Fig. 10 shows the HER activity of the modified electrocatalyst with the overpotential value of 496 mV at the current density of 10 $mAcm^{-2}$. HER in alkaline media required a higher overpotential value than the acidic

Table 1
Electrochemical parameters for the CNTs fiber-based electrocatalysts toward OER.

Electrocatalysts	η_{10} (mV)	η_{100} (mV)	Tafel slope ($mVdec^{-1}$)	R_{ct} (Ω)	C_{dl} (μF)	ECSA (cm^2)
Bare CNTs fiber (OER)	–	–	243.0	1200	8	0.20
CoSe@CNTs fiber (OER)	414	494	77.0	57	166	4.15
CoSe@CNTs fiber (Overall water splitting)	540	590	102.6	73	–	–

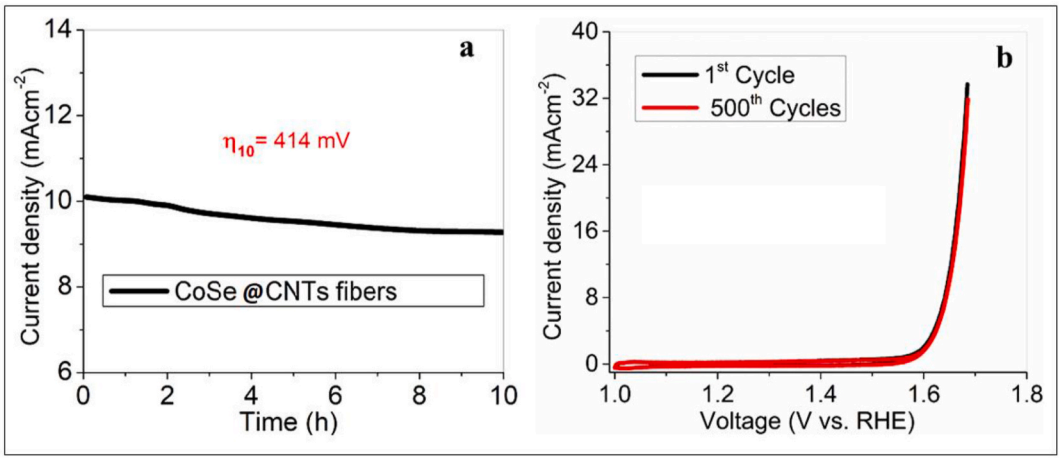

Fig. 9. (a) Chronoamperometric measurement of long-term stability of CoSe@CNTs fiber at the current density of 10 mA cm^{-2} for 10 h and **(b)** comparison of 1st and 500th CV cycles.

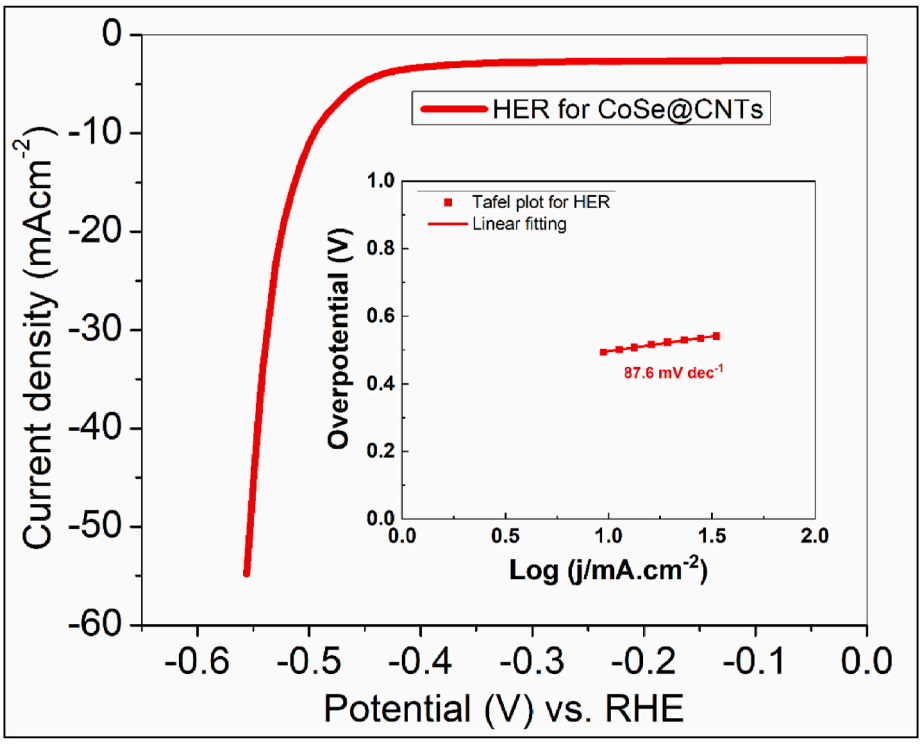

Fig. 10. *iR*-corrected polarization curve for the modified CoSe@CNTs fiber electrode for HER in aqueous 1 M KOH solution at the scan rate of 5 mVs^{-1}. The inset shows the Tafel slope.

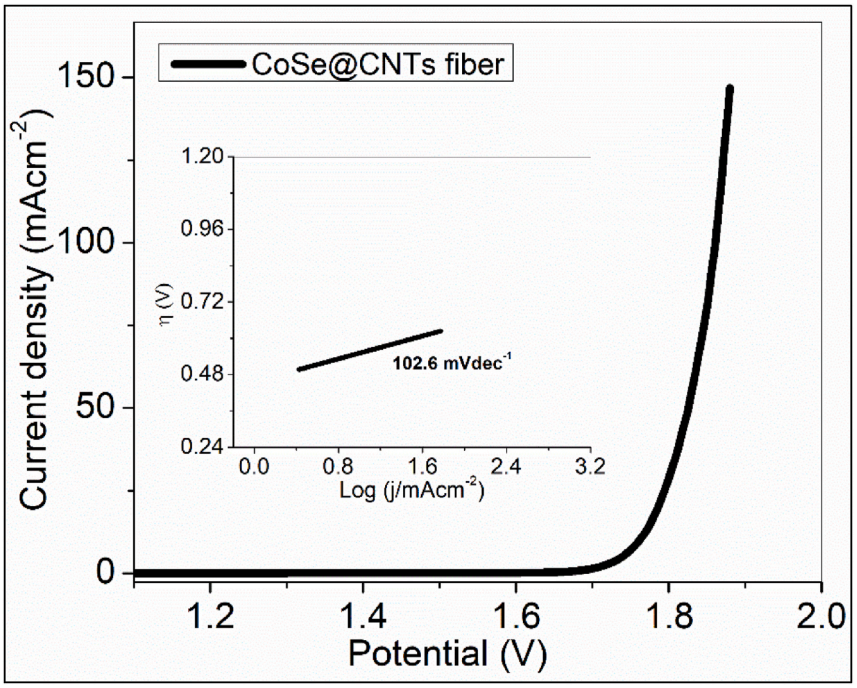

Fig. 11. *iR*-corrected polarization curve of the modified CoSe@CNTs fiber for overall water splitting in aqueous 1 M KOH solution. The inset shows the Tafel slope.

media which is due to the initial water splitting procedure in the Volmer step. This step activates the H* by cleaving the H-O-H bond and is considered to be the rate-determining step in the overall electrochemical water splitting reaction [48]. A higher value of Tafel slope (87.6 $mVdec^{-1}$), given as inset of Fig. 10, also implies the sluggish hydrogen evolution at the cathode surface in the presence of OH^- ions. Inclusively, the fabricated electrode showed the multidimensional activities towards OER, HER and overall electrochemical water splitting reactions in alkaline media.

3.2.3. *Overall electrochemical water splitting*

We also assessed the overall water splitting by replacing the Pt electrode with the modified CNTs fiber electrode that served as a cathode, in addition to using it as an anode. The outcome showed the

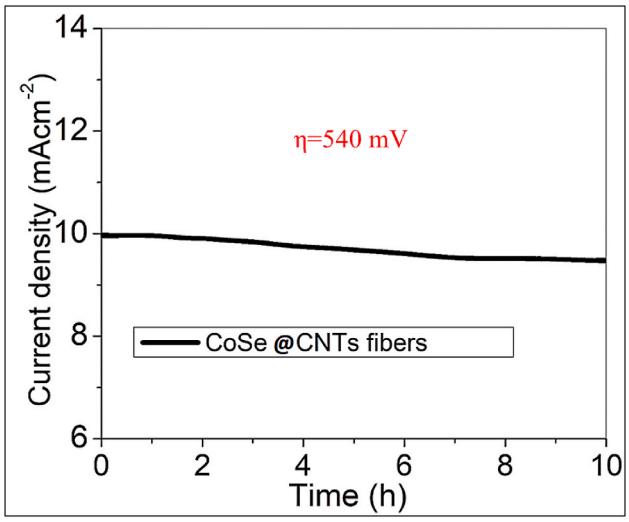

Fig. 12. Chronoamperometric studies for the durability of CoSe@CNTs fiber electrode at 540 mV overpotential for overall water splitting.

reasonable performance of the fabricated electrode as shown in the polarization curve (Fig. 11). With the replacement of Pt metal at the counter electrode, overpotential values slightly increased to 540 and 590 mV corresponding to the current density of 10 and 100 $mAcm^{-2}$, respectively. The Tafel slope (inset plot in Fig. 11) derived for the modified electrode is calculated to be 102.6 $mVdec^{-1}$ which also demonstrates the fast kinetics of the process. The results reveal that the strong synergistic effect of high activity by CoSe along with the faster charge transfer ability of CNTs fiber resulted in faster charge transfer kinetics and enhanced electrochemical water splitting of CoSe@CNTs fiber.

Fig. 12 represents the long-term stability for overall water splitting by finding the current density at a fixed potential (540 mV) for 10 h. It has been observed that the current response by modified fiber is quite stable for the specified time and a well-maintained faradaic process was observed for the period of 10 h. A post-SEM analysis was also performed to check the catalytic behavior of the used materials as shown in Fig. S5 in supporting information. A slight modification of the electrode was observed that may lead to a decrease in catalytic active sites and hence a slight decrease in current density over time.

4. Conclusion

We reported a flexible and knittable fiber-structured electrocatalyst for overall electrochemical water splitting. A single-step hydrothermal method was used for the in-situ growth of CoSe nanoparticles over the surface CNTs fiber which was deployed as an electrode material in water electrolysis. Surface morphology and elemental analysis were performed that illustrated a clear picture of nanoparticle deposition and their uniform distribution over the fiber surface. Overpotential values for water oxidation, along with overall splitting, are found to be closer to the thermodynamic water oxidation potential. The electrocatalyst was also examined for the HER within the cathodic region under alkaline media, showing reasonable activity. Higher double-layer capacitance and lower charge transfer resistance were also calculated via CV and EIS, respectively, and are found to be improved for the modified fiber as compared to that of pristine CNTs fiber. As demonstrated, the fabricated flexible microelectrodes could be utilized as a highly efficient, stable and multidimensional electrocatalyst in flexible energy conversion systems.

Declaration of competing interest

The authors declare that they have no known competing financial interests or personal relationships that could have appeared to influence the work reported in this paper.

Acknowledgments

The authors would like to thank the Deanship of Scientific Research at Shaqra University for supporting this work. The authors are also highly thankful to the Higher Education Commission (HEC) Pakistan for providing financial support for the startup grant (21-2146/SRGP/R&D/HEC/2018) and Prof. Dr. Huisheng Peng from the Fudan University China, for providing the facilities for the growth of carbon nanotubes fibers. Z.I is also thankful to Deutscher Akademischer Austauschdienst (DAAD) for a Ph.D. scholarship to study at HZB.

Appendix A. Supplementary data

Supplementary data to this article can be found online at https://doi.org/10.1016/j.jsamd.2023.100638.

References

[1] X. Wang, H. Huang, J. Qian, Y. Li, K. Shen, Intensified Kirkendall effect assisted construction of double-shell hollow Cu-doped CoP nanoparticles anchored by carbon arrays for water splitting, Appl. Catal. B Environ. 325 (2023) 122295.
[2] X. Zhang, H. Zhao, C. Li, S. Li, K. Liu, L. Wang, Facile coordination driven synthesis of metal-organic gels toward efficiently electrocatalytic overall water splitting, Appl. Catal. B Environ. 299 (2021) 120641.
[3] B.S. Reghunath, S. Rajasekaran, S. Devi K R, D. Pinheiro, J.R. Jaleel Uc, N-doped graphene quantum dots incorporated cobalt ferrite/graphitic carbon nitride ternary composite for electrochemical overall water splitting, Int. J. Hydrogen Energy 48 (2023) 2906–2919.
[4] R. Miao, B. Dutta, S. Sahoo, J. He, W. Zhong, S.A. Cetegen, T. Jiang, S.P. Alpay, S. L. Suib, Mesoporous iron sulfide for highly efficient electrocatalytic hydrogen evolution, J. Am. Chem. Soc. 139 (2017) 13604–13607.
[5] T. Reier, M. Oezaslan, P. Strasser, Electrocatalytic oxygen evolution reaction (OER) on Ru, Ir, and Pt catalysts: a Comparative study of nanoparticles and Bulk materials, ACS Catal. 2 (2012) 1765–1772.
[6] W. Li, J. Liu, D. Zhao, Mesoporous materials for energy conversion and storage devices, Nat. Rev. Mater. 1 (2016) 16023.
[7] M. Gryszel, M. Sytnyk, M. Jakešová, G. Romanazzi, R. Gabrielsson, W. Heiss, E. D. Głowacki, General Observation of Photocatalytic oxygen reduction to hydrogen Peroxide by organic Semiconductor thin films and Colloidal Crystals, ACS Appl. Mater. Interfaces 10 (2018) 13253–13257.
[8] J. Barber, Hydrogen derived from water as a sustainable solar fuel: learning from biology, Sustain. Energy Fuels 2 (2018) 927–935.
[9] P. Yu, J. Ma, R. Zhang, J.Z. Zhang, G.G. Botte, Novel Pd–Co electrocatalyst supported on carbon fibers with enhanced electrocatalytic activity for coal electrolysis to produce hydrogen, ACS Appl. Energy Mater. 1 (2018) 267–272.
[10] W. Zhou, S. Chen, X. Meng, J. Li, J. Gao, Energy-saving cathodic H_2 production enabled by non-oxygen evolution anodic reactions: a critical review on fundamental principles and applications, Int. J. Hydrogen Energy 48 (2023) 15748–15770.
[11] S. Battiato, A.L. Pellegrino, A. Pollicino, A. Terrasi, S. Mirabella, Composition-controlled chemical bath deposition of Fe-doped NiO microflowers for boosting oxygen evolution reaction, Int. J. Hydrogen Energy 48 (2023) 18291–18300.
[12] F. Zhou, L. Zhang, J. Li, Q. Wang, Y. Chen, H. Chen, G. Lu, G. Chen, H. Jin, S. Wang, J. Wang, Novel engineering of ruthenium-based electrocatalysts for acidic water oxidation: a mini review, Engineering Reports 3 (2021), e12437.
[13] J. Yu, Q. He, G. Yang, W. Zhou, Z. Shao, M. Ni, Recent Advances and Prospective in ruthenium-based materials for electrochemical water splitting, ACS Catal. 9 (2019) 9973–10011.
[14] Z. Chen, X. Duan, W. Wei, S. Wang, B.-J. Ni, Iridium-based nanomaterials for electrochemical water splitting, Nano Energy 78 (2020) 105270.
[15] Y. Yang, Y. Yu, J. Li, Q. Chen, Y. Du, P. Rao, R. Li, C. Jia, Z. Kang, P. Deng, Y. Shen, X. Tian, Engineering ruthenium-based electrocatalysts for effective hydrogen evolution reaction, Nano-Micro Lett. 13 (2021) 160.
[16] X.-P. Li, C. Huang, W.-K. Han, T. Ouyang, Z.-Q. Liu, Transition metal-based electrocatalysts for overall water splitting, Chin. Chem. Lett. 32 (2021) 2597–2616.
[17] M. Herbaut, M. Siaj, J.P. Claverie, Nanomaterials-based water splitting: How far are We from a sustainable solution? ACS Appl. Nano Mater. 4 (2021) 907–910.
[18] J. Yu, T.A. Le, N.Q. Tran, H. Lee, Earth-abundant transition-metal-based bifunctional electrocatalysts for overall water splitting in alkaline media, Chem. Eur J. 26 (2020) 6423–6436.
[19] L. Zhang, Q. Fan, K. Li, S. Zhang, X. Ma, First-row transition metal oxide oxygen evolution electrocatalysts: regulation strategies and mechanistic understandings, Sustain. Energy Fuels 4 (2020) 5417–5432.
[20] F. Lu, M. Zhou, Y. Zhou, X. Zeng, First-row transition metal based catalysts for the oxygen evolution reaction under alkaline conditions: basic principles and recent advances, Small 13 (2017), 1701931.

[21] Q. Zhai, Y. Pan, L. Dai, Carbon-based metal-Free electrocatalysts: Past, present, and Future, Acc. Mater. Res. 2 (2021) 1239–1250.
[22] Z. Zhang, Y. Lei, W. Huang, Recent progress in carbon-based materials boosting electrochemical water splitting, Chin. Chem. Lett. 33 (2021) 3623–3631.
[23] Q. Hu, G. Li, Z. Han, Z. Wang, X. Huang, H. Yang, Q. Zhang, J. Liu, C. He, Recent progress in the hybrids of transition metals/carbon for electrochemical water splitting, J. Mater. Chem. A 7 (2019) 14380–14390.
[24] W. Li, C. Wang, X. Lu, Integrated transition metal and compounds with carbon nanomaterials for electrochemical water splitting, J. Mater. Chem. A 9 (2021) 3786–3827.
[25] J. Zhang, Z. Xia, L. Dai, Carbon-based electrocatalysts for advanced energy conversion and storage, Sci. Adv. 1 (2015), e1500564.
[26] C. Hu, Y. Xiao, Y. Zou, L. Dai, Carbon-based metal-Free electrocatalysis for energy conversion, energy storage, and environmental Protection, Electrochem. Energy Rev. 1 (2018) 84–112.
[27] J. Deng, P. Ren, D. Deng, X. Bao, Enhanced electron Penetration through an Ultrathin graphene layer for highly efficient Catalysis of the hydrogen evolution reaction, Angew. Chem. Int. Ed. 54 (2015) 2100–2104.
[28] Y. Yang, Z. Lin, S. Gao, J. Su, Z. Lun, G. Xia, J. Chen, R. Zhang, Q. Chen, Tuning electronic structures of Nonprecious ternary alloys encapsulated in graphene layers for Optimizing overall water splitting activity, ACS Catal. 7 (2017) 469–479.
[29] A.L.M. Reddy, S. Ramaprabhu, Nanocrystalline metal oxides dispersed multiwalled carbon nanotubes as Supercapacitor electrodes, J. Phys. Chem. C 111 (2007) 7727–7734.
[30] N.I. Andersen, A. Serov, P. Atanassov, Metal oxides/CNT nano-composite catalysts for oxygen reduction/oxygen evolution in alkaline media, Appl. Catal. B Environ. 163 (2015) 623–627.
[31] X. Liu, W. Liu, M. Ko, M. Park, M.G. Kim, P. Oh, S. Chae, S. Park, A. Casimir, G. Wu, J. Cho, Metal (Ni, Co)-Metal oxides/graphene nanocomposites as multifunctional electrocatalysts, Adv. Funct. Mater. 25 (2015) 5799–5808.
[32] Y. Ouyang, Q. Li, L. Shi, C. Ling, J. Wang, Molybdenum sulfide clusters immobilized on defective graphene: a stable catalyst for the hydrogen evolution reaction, J. Mater. Chem. A 6 (2018) 2289–2294.
[33] N. Wang, L. Li, D. Zhao, X. Kang, Z. Tang, S. Chen, Graphene composites with cobalt sulfide: efficient trifunctional electrocatalysts for oxygen reversible Catalysis and hydrogen production in the same electrolyte, Small 13 (2017), 1701025.
[34] A. Ashok, A. Kumar, J. Ponraj, S.A. Mansour, Development of Co/Co9S8 metallic nanowire anchored on N-doped CNTs through the pyrolysis of melamine for overall water splitting, Electrochim. Acta 368 (2021) 137642.
[35] Y. Shi, D. Zhang, H. Miao, W. Zhang, X. Wu, Z. Wang, H. Li, T. Zhan, X. Chen, J. Lai, L. Wang, A simple, rapid and scalable synthesis approach for ultra-small size transition metal selenides with efficient water oxidation performance, J. Mater. Chem. A 9 (2021) 24261–24267.
[36] H. Singh, M. Marley-Hines, S. Chakravarty, M. Nath, Multi-walled carbon nanotube supported manganese selenide as a highly active bifunctional OER and ORR electrocatalyst, J. Mater. Chem. A 10 (2022) 6772–6784.
[37] B. Hu, X. Liu, A. Liu, Y. Ren, Z. Guo, J. Mu, X. Zhang, Z. Zhang, X. Liu, H. Che, Reduced graphene oxide Nanosheet-Wrapped hollow cobalt selenide Nanocubes as electrodes for Supercapacitors, ACS Appl. Nano Mater. 4 (2021) 13267–13278.
[38] D. Xu, X. Long, Juanxiu Xiao, Z. Zhang, G. Liu, H. Tong, Z. Liu, N. Li, D. Qian, J. Li, J. Liu, Rationally constructing CoO and $CoSe_2$ hybrid with CNTs-graphene for impressively enhanced oxygen evolution and DFT calculations, Chem. Eng. J. 422 (2021) 129982.
[39] M. Zhu, X. Bai, Q. Yan, Y. Yan, K. Zhu, K. Ye, J. Yan, D. Cao, X. Huang, G. Wang, Iron molybdenum selenide supported on reduced graphene oxide as an efficient hydrogen electrocatalyst in acidic and alkaline media, J. Colloid Interface Sci. 602 (2021) 384–393.
[40] A. Vazhayil, L. Vazhayal, J. Thomas, S. Ashok C, N. Thomas, A comprehensive review on the recent developments in transition metal-based electrocatalysts for oxygen evolution reaction, Appl. Surf. Sci. Adv. 6 (2021) 100184.
[41] R. Paul, L. Zhu, H. Chen, J. Qu, L. Dai, Recent Advances in carbon-based metal-Free electrocatalysts, Adv. Mater. 31 (2019), 1806403.
[42] G. Liu, C. Shuai, Z. Mo, R. Guo, N. Liu, X. Niu, Q. Dong, J. Wang, Q. Gao, Y. Chen, W. Liu, The one-pot synthesis of porous Ni0.85Se nanospheres on graphene as an efficient and durable electrocatalyst for overall water splitting, New J. Chem. 44 (2020) 17313–17322.
[43] P. Xu, J. Zhang, Z. Ye, Y. Liu, T. Cen, D. Yuan, Co doped Ni0.85Se nanoparticles on RGO as efficient electrocatalysts for hydrogen evolution reaction, Appl. Surf. Sci. 494 (2019) 749–755.
[44] W. Hou, B. Zheng, F. Qi, B. Yu, Y. Chen, Self-assembled CNT/Ni0.85Se-SnO2 networks as highly efficient and stable electrocatalyst for hydrogen evolution reaction, Electrochim. Acta 269 (2018) 155–162.
[45] Y. Zhang, T. Ye, L. Li, H. Peng, Carbon nanotubes for flexible fiber Batteries, in: F. Borghi, F. Soavi, P. Milani (Eds.), Nanoporous Carbons for Soft and Flexible Energy Devices, Springer International Publishing, Cham, 2022, pp. 1–22.
[46] L. Qiu, Q. Wu, Z. Yang, X. Sun, Y. Zhang, H.J.S. Peng, Freestanding aligned carbon nanotube array grown on a large-area single-layered graphene sheet for efficient dye-sensitized, solar cell, Small 11 (2015) 1150–1155.
[47] A. Sivanantham, P. Ganesan, L. Estevez, B.P. McGrail, R.K. Motkuri, S. Shanmugam, A stable graphitic, Nanocarbon-encapsulated, cobalt-rich Core–shell electrocatalyst as an oxygen electrode in a water electrolyzer, Adv. Energy Mater. 8 (2018), 1702838.
[48] J. Wei, M. Zhou, A. Long, Y. Xue, H. Liao, C. Wei, Z.J. Xu, Heterostructured electrocatalysts for hydrogen evolution reaction under alkaline conditions, Nano-Micro Lett. 10 (2018) 75.